

# Towards Robust Perception: A Framework for Combining Point Clouds from Multiple LiDARs

C.A. Rakshith Ram<sup>1</sup>, Abhishek Thakur<sup>2</sup>, and P. Rajalakshmi<sup>2</sup>

<sup>1</sup>Center for Interdisciplinary Programs, <sup>2</sup>Department of Electrical Engineering,

Indian Institute of Technology Hyderabad, India

email: sm22mtech12003@iith.ac.in, ee20resch11014@iith.ac.in, raji@ee.iith.ac.in

**Abstract**—The increasing deployment of autonomous systems in complex environments demands robust perception capabilities. Light Detection and Ranging (LiDAR) sensors, while critical for providing high-resolution spatial data, often face coverage limitations, leading to blind spots. This paper presents a novel framework that mitigates these blind spots, which are prominent when using a single LiDAR, by integrating point clouds from multiple strategically placed LiDARs. Our method eliminates the need for complex external calibration by employing Temporal and Spatial alignment techniques to construct a comprehensive environmental representation. This approach effectively addresses alignment challenges and reduces blind spots. Experimental results show significant improvements in spatial coverage, object detection, and environmental understanding without compromising localization. The proposed scalable framework enhances the perception capabilities of autonomous systems, contributing to safer and more reliable operations.

**Index Terms**—LiDAR, Perception, Blind spots, Temporal Alignment, Spatial Alignment, Localization.

## I. INTRODUCTION

Ensuring robust perception systems is crucial for the safety and reliability of evolving autonomous vehicles. Light Detection and Ranging (LiDAR) sensors are pivotal in this regard, generating high-resolution 3D point cloud data essential for accurate environmental mapping and perception [1]. Despite their importance, traditional LiDAR setups typically mounted on the front or top of vehicles have notable limitations. These configurations can create significant blind spots, particularly in the rear and lateral areas of the vehicle, increasing the risk of undetected obstacles, especially in dynamic and complex environments.

To address these limitations, we propose a multi-LiDAR sensor configuration to provide a comprehensive 360-degree view of the vehicle's surroundings. By strategically positioning LiDAR sensors around the vehicle, as depicted in Fig. 1, our approach aims to effectively eliminate blind spots and enhance obstacle detection from all directions [2]. This multi-LiDAR setup improves situational awareness and supports more accurate decision-making and navigation, which is critical for safe and reliable autonomous driving.

In this paper, we introduce a novel framework as outlined in Fig. 2, for integrating point clouds from multiple LiDAR sensors. Our framework tackles the challenges associated with sensor calibration, data fusion, and real-time processing. By addressing these key issues, our approach enhances the perception capabilities of autonomous vehicles, paving the way

for safer and more reliable operations across various driving scenarios.

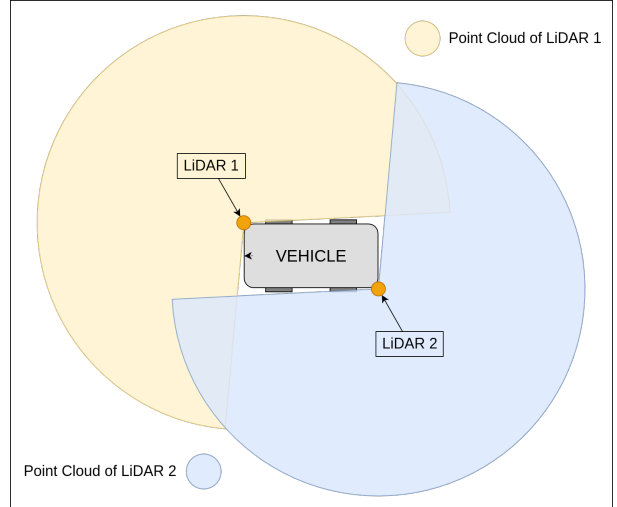


Fig. 1. Achieving full 360-degree coverage by fusing data from two LiDAR sensors.

## II. LITERATURE SURVEY

Multiple LiDAR sensors achieve a 360-degree field of view, enabling effective environment perception, mapping, and localization. In [3], the authors conduct a performance evaluation of ten distinct 3D LiDAR sensor models, such as the VLP-16, VLP-32, HDL-64, and VLS-128 Velodyne LiDARs, focusing on their suitability for automated driving applications. In [4], the authors investigate the characterization of multiple 3D LiDAR (Light Detection and Ranging) systems for their effectiveness in localization and mapping tasks. In [5], the author employed a single front-facing LiDAR for obstacle detection and tracking. However, this approach fails to detect obstacles approaching from the sides and rear, which poses a significant safety risk for autonomous vehicles. A dataset from 10 different LiDAR sensors was collected, with data from one LiDAR sensor captured at each instance in [6]. A framework for multiple LiDAR calibration is discussed in [7]. Using a single front-facing LiDAR for localization results in occlusions on both the rear and front sides [9]. By reducing these blind spots by calibrating two LiDAR sensors, as discussed in this

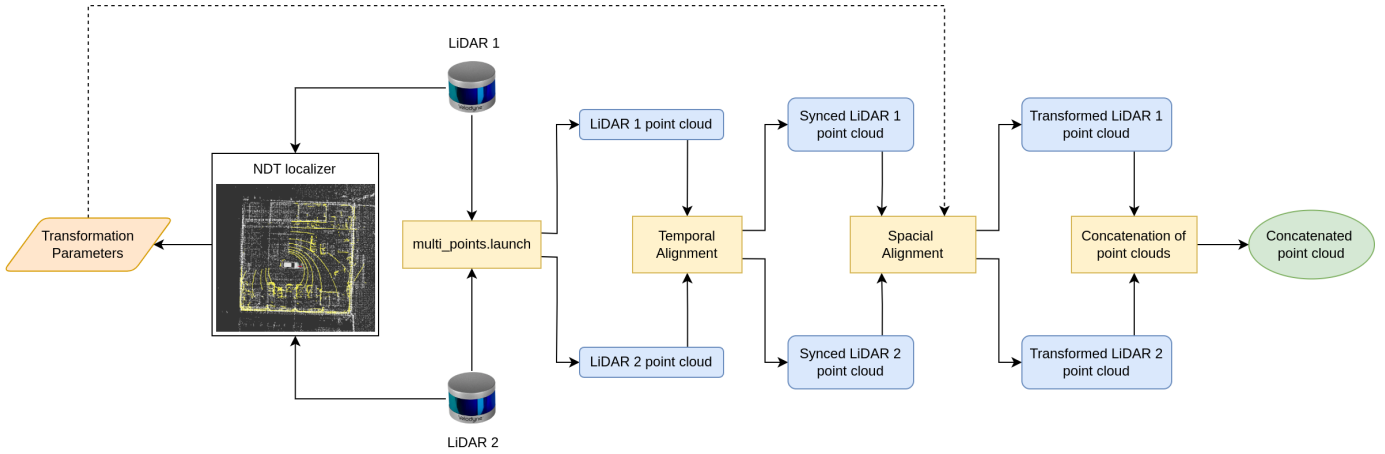


Fig. 2. Flowchart depicting all the steps in the algorithm.

work, more features can be detected, leading to improved perception.

### III. METHODOLOGY

#### A. Strategic Mounting of LiDAR sensor

Initially, the sensors were mounted at a higher position on the vehicle; they created significant blind spots, especially in the lower regions surrounding the vehicle or when an object was passing close to it.

To address this, we have employed an additional LiDAR and systematically lowered the mounting height to 1m from the ground (refer Table I). This adjustment allowed the sensors to capture more of the vehicle's immediate environment, particularly previously obscured areas. By optimizing the height, we ensured that the LiDARs could better detect objects closer to the ground, substantially reducing the overall blind spot radius.

To quantitatively analyze the amount of blind spots reduced. We can measure the radius  $R$  of the blind spot circle in front of the vehicle on a virtual line at a height  $h$  above the ground, as shown in Fig. 3.  $H$  is the height of the mounted LiDAR, and  $\theta$  is the FOV angle below the horizontal.

$$R = (H - h) / \tan(\theta) \quad (1)$$

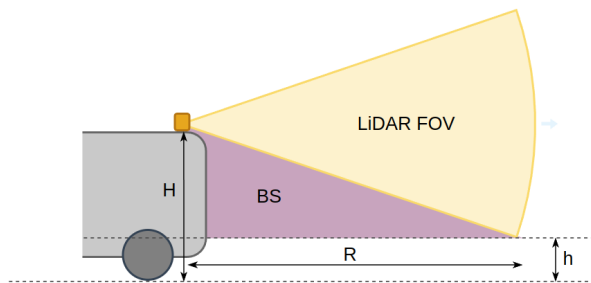


Fig. 3. Depiction of LiDAR mounted on the vehicle, its FOV and blind spot.

#### B. Data Acquisition

To effectively utilize data from multiple LiDAR sensors, it is crucial to manage the data streams individually and accurately, especially when using similar sensors, in this case, two Velodyne VLP16 units. Using the available web interface for the Velodyne LiDARs, the Field of View (FOV) is adjusted to suit our needs. Here, the FOV of each LiDAR is set to  $260^\circ$  as shown in Fig. 1 to have a small clearance with the vehicle body. Distinct values are assigned to the "Data Port" and the "Telemetry Port" to avoid data conflict.

In this framework, the launch files of the Velodyne LiDARs are customized to publish data on distinct ROS topics, in this case, "/node1/velodyne\_points" and "/node2/velodyne\_points". This configuration ensures that each sensor's data is collected and processed independently, providing clarity and flexibility in handling the input streams while avoiding potential conflicts or overlaps.

#### C. LiDAR Pose extraction concerning a Global Reference

To achieve 360-degree perception and minimize blind spots, LiDARs are strategically mounted on opposite corners of the vehicle at an optimal height, as shown in Fig. 5. Before spatially aligning their point clouds, it is crucial to determine each LiDAR's pose relative to a common global reference frame.

To achieve this, an HD map is first generated using the ALOAM algorithm [8], with a temporary LiDAR mounted on the vehicle. The Normal Distributions Transform (NDT) localization algorithm [9] is then used to extract the  $x$ ,  $y$ , and  $z$  parameters from the "/ndt\_pose" topic and the roll, pitch, and yaw parameters from the "/euler\_angle" topic for both LiDARs.

$$\text{pose\_1} = [x_1, y_1, z_1, \phi_1, \theta_1, \psi_1] \quad (2)$$

$$\text{pose\_2} = [x_2, y_2, z_2, \phi_2, \theta_2, \psi_2] \quad (3)$$

These pose parameters are essential inputs for the subsequent spatial alignment, ensuring accurate data integration and reliable perception.

#### D. Temporal Alignment of LiDAR Data

In processing data from multiple LiDARs, accurate time synchronization is essential for reliable subsequent analysis. To achieve this, the "ApproximateTime" policy in ROS was utilized. This policy synchronizes messages based on their timestamps within a defined tolerance, accommodating minor timing differences between sensors.

By employing the Approximate Time policy, the framework ensures that LiDAR data streams are aligned within a reasonable time window. This approach effectively handles timing discrepancies due to network delays or sensor clock variations, providing a temporally coherent dataset for further processing.

#### E. Spatial Alignment and Concatenation



Fig. 4. Data (point clouds) from both the LiDARs after Spatial alignment covering complete 360° field of view.

We input the extracted pose parameters into our transformation package, applying the necessary transformations to each point cloud. This process, detailed in the equations below, achieves extrinsic calibration by aligning the point clouds with the global reference frame.

$$\mathbf{R} = \mathbf{R}_z(\psi) \cdot \mathbf{R}_y(\theta) \cdot \mathbf{R}_x(\phi) \quad (4)$$

$$\mathbf{T} = [t_x \quad t_y \quad t_z]^T \quad (5)$$

$$\mathbf{M} = \begin{bmatrix} \mathbf{R} & \mathbf{T} \\ 0 & 1 \end{bmatrix} \quad (6)$$

$$\mathbf{p}_i = [x_i \quad y_i \quad z_i \quad 1]^T \quad (7)$$

$$\mathbf{p}_i' = \mathbf{M} \cdot \mathbf{p}_i \quad (8)$$

Here,  $\mathbf{R} \in \mathbb{R}^{3 \times 3}$  is the rotation matrix (with  $\psi, \phi, \theta$  as roll, pitch, and yaw), and  $\mathbf{T} \in \mathbb{R}^{3 \times 1}$  is the translation matrix. Together, they form the transformation matrix  $M$ , used to convert

each point  $p_i$  to its new position  $p'_i$ . To merge the transformed point clouds, we use the `pcl::concatenatePointCloud` function from the Point Cloud Library (PCL). This function efficiently combines multiple point clouds into a single dataset, ensuring consistency across data fields. This method is widely used in 3D reconstruction, sensor fusion, and environmental modelling. After transformation, the point clouds are concatenated, resulting in a comprehensive 360-degree perception of the vehicle's surroundings. While some overlap between LiDAR1 and LiDAR2 exists, it enhances overall perception without impacting intended applications.

## IV. RESULTS AND ANALYSIS

This section explores our framework's practical applications and experimental validation for combining point clouds from multiple LiDAR sensors. Utilizing the concatenated LiDAR data shown in Fig. 4, we conducted localization, navigation and obstacle detection tasks, resulting in improved environmental perception and reduced blind spots.

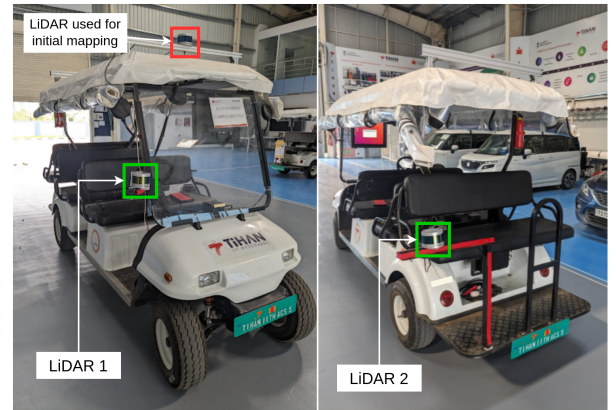


Fig. 5. LiDARs mounted on a test vehicle for experimentation.

#### A. Localization and Navigation

Experiments were conducted using a vehicle (shown in Fig. 5) to realise the application of the concatenated point cloud for localization and navigation in an autonomous vehicle test facility, TiHAN [10]. The NDT localizer algorithm matched the point cloud against a prebuilt high-definition map, achieving localization, as shown in Fig. 6. Autonomous navigation was also performed using the same point cloud within the facility. The rich data from the concatenated LiDARs ensured precise position estimation, even in scenarios with occlusions or limited visibility, which is vital for autonomous navigation and other perception-driven tasks.

#### B. Enhanced Perception

A significant outcome of our multi-LiDAR setup was the substantial reduction in blind spots around the vehicle. The reduction of blind spots enhanced the safety and reliability of the system, especially in dynamic environments where complete situational awareness is critical. The comprehensive point cloud generated by the concatenated LiDAR data provided a

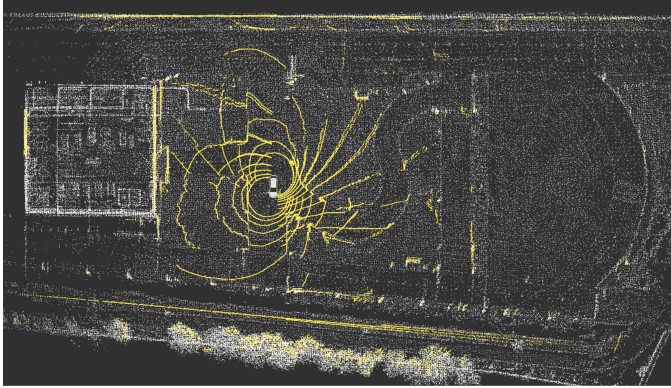


Fig. 6. Visualization of successful localization using the concatenated point clouds on a HD map of the TiHAN testbed [10].

more holistic 360° field view of the surroundings, contributing to better decision-making and obstacle detection and avoidance as shown in Fig. 7. The approximate area of blindspot, taking into consideration two LiDAR sensors and the 260° FOV, is given by,

$$A = 2 * \pi * R^2 * (260/360) \quad (9)$$

Using equations 1 and 9, the approximate area of blindspot, varying with H for the setup, is given in table I:

TABLE I  
VARIATION OF THE BLINDSPOT AREA WITH RESPECT TO THE HEIGHT OF  
LiDAR MOUNTING.

H (m)	R (m)	Blind spot area (m <sup>2</sup> )
0.75	0.93	3.95
1.00	1.86	15.80
1.25	2.80	35.55
1.50	3.73	63.20
1.75	4.66	98.75
2.00	5.59	142.21

Overall, the experimental results demonstrate the effectiveness of our framework in enhancing LiDAR-based perception while not affecting other applications, such as localization and navigation, as validated in real-time tests on the TiHAN testbed [10].

## CONCLUSION

This paper introduces a framework for enhancing autonomous vehicle perception by integrating multiple LiDAR sensors, significantly improving coverage and reducing blind spots. By optimizing sensor placement and applying advanced data fusion techniques, our approach achieves a comprehensive 360-degree view around the vehicle. This enhancement improves obstacle-detection capabilities while not affecting localization and navigation. Our experimental results demonstrate the framework's effectiveness in providing a robust and reliable perception system, with notable reductions in blind spots. Future research may focus on improving sensor calibration,

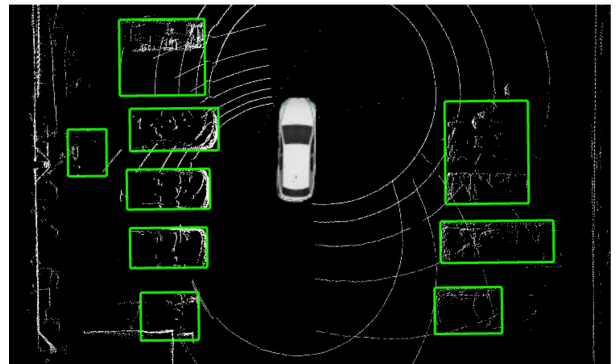


Fig. 7. Perception task realized using the concatenated point cloud.

improving real-time data processing, and exploring additional applications to advance autonomous vehicle technology.

## ACKNOWLEDGMENT

This work is supported by the DST National Mission Interdisciplinary Cyber-Physical Systems (NM-ICPS), Technology Innovation Hub on Autonomous Navigation and Data Acquisition Systems: TiHAN Foundation at Indian Institute of Technology (IIT) Hyderabad.

## REFERENCES

- [1] H. Wang, C. Wang, C. -L. Chen and L. Xie, "F-LOAM : Fast LiDAR Odometry and Mapping," 2021 IEEE/RSJ International Conference on Intelligent Robots and Systems (IROS), Prague, Czech Republic, 2021, pp. 4390-4396, doi: 10.1109/IROS51168.2021.9636655.
- [2] L. -J. Kau, L. -J. Chiou, Y. -H. Lo and S. -H. Chen, "A Multi-Lidar-based Point Cloud Acquisition Platform and Data Fusion for Autonomous Vehicle in Complex Urban Environment," 2023 IEEE International Symposium on Circuits and Systems (ISCAS), Monterey, CA, USA, 2023, pp. 1-5, doi: 10.1109/ISCAS46773.2023.10181581.
- [3] Lambert J, Carballo A, Cano AM, Narksri P, Wong D, Takeuchi E, Takeda K, "Performance analysis of 10 models of 3D LiDARs for automated driving", 2020 IEEE Access. PP. 1-1. 10.1109/ACCESS.2020.3009680
- [4] A. Carballo et al., "Characterization of Multiple 3D LiDARs for Localization and Mapping Performance using the NDT Algorithm," 2021 IEEE Intelligent Vehicles Symposium Workshops (IV Workshops), Nagoya, Japan, 2021, pp. 327-334, doi: 10.1109/IVWorkshops54471.2021.9669244.
- [5] A. Thakur and P. Rajalakshmi, "L3D-OTVE: LiDAR-Based 3-D Object Tracking and Velocity Estimation Using LiDAR Odometry," IEEE Sensors Letters, vol. 8, no. 7, pp. 1-4, July 2024, Art no. 6008004, doi: 10.1109/LSENS.2024.3416411.
- [6] A. Carballo et al., "LIBRE: The Multiple 3D LiDAR Dataset," 2020 IEEE Intelligent Vehicles Symposium (IV), Las Vegas, NV, USA, 2020, pp. 1094-1101, doi: 10.1109/IV47402.2020.9304681.
- [7] J. Lin, X. Liu and F. Zhang, "A decentralized framework for simultaneous calibration, localization and mapping with multiple LiDARs," 2020 IEEE/RSJ International Conference on Intelligent Robots and Systems (IROS), Las Vegas, NV, USA, 2020, pp. 4870-4877, doi: 10.1109/IROS45743.2020.9340790.
- [8] A. Thakur, B. Anand, H. Verma and P. Rajalakshmi, "Real Time Lidar Odometry and Mapping and Creation of Vector Map," 2022 8th International Conference on Automation, Robotics and Applications (ICARA), Prague, Czech Republic, pp. 181-185, 2022.
- [9] A. Thakur and P. Rajalakshmi, "LiDAR-Based Optimized Normal Distribution Transform Localization on 3-D Map for Autonomous Navigation," IEEE Open Journal of Instrumentation and Measurement, vol. 3, pp. 1-11, 2024, Art no. 8500211, doi: 10.1109/OJIM.2024.3412219.
- [10] TiHAN: TiHAN IIIT Autonomous Navigation Testbed [Online]. Available: <https://tihan.iith.ac.in/>